DATA PROCESSING OF VU C-BAND POLARIMETRIC RADAR

8

Raquel Evaristo, Teresa Bals-Elsholz and Adam Stepanek

Valparaiso University, Valparaiso, Indiana, USA

1. Introduction

The Valparaiso University Meteorology Department owns a C-band polarimetric radar. The geographic location of the radar, approximately 20 km south of Lake Michigan, in Northwest Indiana, allows the observation of several different types of weather, from mid-latitude winter cyclones producing snow, to more local events like lake effect snow/rain, mesoscale convective systems often producing severe weather, etc. Because of the close proximity to the lake, there is a strong spatial variability in atmospheric conditions, and the presence of the radar in this strategic location is of great importance in the observation of certain storm features that would otherwise be missed.

Some of the usage of radar requires high accuracy of the radar variables. For example, precipitation estimation requires an accuracy of 1dBZ in reflectivity for an accuracy of 15% (Gourley *et al*., 2009). Radar measurements may be affected by errors such as calibration (in reflectivity (Z_h) and differential reflectivity (Z_{dr})), attenuation and differential attenuation.

This paper describes the methods we use to correct for these errors and illustrates the different steps in the procedures.

2. Calibration

Z_{dr} is calibrated by collecting measurements at vertical incidence in rain, rotating the antenna 360° in azimuth, like described in Gorgucci et al.,1999. The Z_{dr} value in these conditions should be zero, and any observed values different from zero are considered the Zdr bias.

The calibration of Z_H is done using a technique known as self-consistency method, which was first proposed by Gorgucci *et al.*,1992 and later studied/improved by many others (Goddard *et al.*, 1994, Gorgucci *et al.*, 1999, Gourley *et al.*, 2009). This method is based on properties of the polarimetric variables in rain. In fact, within rain medium, Z_H, Z_{DR} and K_{DP} are not independent. Thus, K_{DP} may be calculated from Z_{DR} and Z_H and compared to the actual K_{DP}. The discrepancy between calculated and observed K_{DP} is attributed to the miscalibration of Z_H.

Gourley et al., 2009, found the following relationship between the 3 variables:

$$K_{DP} = Z_H \left[10^{-5}\left(a_0 + a_1 Z_{DR} + a_2 Z_{DR}^{2} + a_3 Z_{DR}^{3}\right)\right], \qquad 1.$$

Where K_{DP} is in ° km^{-1}, Z_H in mm^6 m^{-3} and Z_{DR} in dB.

The coefficients, at C-band are:

a_0= 6.746

a_1= - 2.970

a_2= 0.711

a_3= - 0.079.

Using Z_H and Z_{DR}, a theoretical value for K_{DP} ($K_{DP,th}$) is calculated based on equation 1. By integrating with respect to radar range, a theoretical value for Φ_{DP} is retrieved ($\Phi_{DP,th}$). The actual Φ_{DP} is then compared to $\Phi_{DP,th}$. If both values match, the reflectivity is calibrated. If they don't match we assume the discrepancy is due to the bias in Z_H and we proceed to determine the magnitude of the bias. This is done by adding or subtracting multiples of 0.5dBZ to Z_H and performing the steps described above to obtain different values for $\Phi_{DP,th}$. The bias is eventually determined by finding the $\Phi_{DP,th}$ that minimizes the difference $|\Phi_{DP,th} - \Phi_{DP}|$.

**Corresponding Author: Raquel Evaristo, Valparaiso University, Dep. Of Geography and Meteorology, Kallay-Christopher Hall, 201-A 1809 Chapel Drive, Valparaiso IN, 46383*

e-mail: Raquel.Evaristo@valpo.edu

This procedure is illustrated in figure 1 where Φ_{DP} and several $\Phi_{DP,th}$ are plotted as a function of radar range. The whole process is repeated for each azimuth, so that we have a bias in each direction (figure 2). Theoretically the bias should be the same for each radial, but since that is not what is observed in practice, this is performed to check how strong the fluctuations are. If the variations with azimuth seem reasonable, the reflectivity bias is assumed to be the mean of the biases.

3. Attenuation and Differential Attenuation Correction

At C-band, attenuation and differential attenuation may seriously affect radar measurements.

The differential phase shift (Φ_{DP}) is known to be proportional to the attenuation and differential attenuation, following the relationships:

$$Z_{H,corr} = Z_{H,meas} + \gamma_H \Delta\Phi_{DP} \qquad \text{2.a}$$

$$Z_{DR,corr} = Z_{DR,meas} + \gamma_{DP} \Delta\Phi_{DP}, \qquad \text{2.b}$$

where the subscript “meas” refers to the measured (observed) value of Z_H or Z_{DR}, and the subscript “corr” refers to the value of Z_H or Z_{DR} after correction for attenuation are applied. γ_H and γ_{DP} are the attenuation coefficient and differential attenuation coefficient, respectively. From equations 2.a and 2.b we verify that changes in Z_H and Z_{DR} due to attenuation depend only on the change in Φ_{DP} ($\Delta\Phi_{DP}$) and the coefficients γ. Therefore, the attenuation coefficient (or differential attenuation coefficient) may be calculated from Z_H- Φ_{DP} scatterplots, (or Z_{DR}-Φ_{DP} scatterplots as in figure 3) by finding the best fit to the data. The slopes of the regressions are the attenuation and differential attenuation coefficients.

To ensure that the variations are primarily due to attenuation, we impose a minimum limit of 40dBZ on the calculation of γ_H and γ_{DP}. This method is based on the attenuation method from May et al. 1999. However, instead of finding one γ_H and one γ_{DP} for the whole domain, the calculation of the coefficients is made independently for each radar pulse. We chose to do this because depending on the type of event and the position of the precipitation relative to the radar, the signal may be strongly affected by attenuation in some directions, and significantly less affected in other directions. Using a constant attenuation coefficient throughout the whole domain would probably be underestimating attenuation in some directions and overestimating in others.

Figure 4 shows an example of the calculated γ_H and γ_{DP} in each direction. They correspond to the reflectivity and differential reflectivity images in figure 5a and 5c. The region to the southeast, where no precipitation is occurring at this point, shows very weak coefficients for both Z_H and Z_{DR}, while strong coefficients are retrieved in the west or northwest, where there is convection.

Figure 5 shows the comparison between the observed and corrected variables: 5a and 5b show Z_H before and after the correction, and 5c and 5d show Z_{DR} before and after correction. The event is a linear convective system, oriented approximately from northeast to southwest. The strong convection along the leading edge of the system is responsible for the attenuation in the trailing stratiform region. As seen in figures 5a and 5b, to the west of the radar, Z_H is about 5 dBZ stronger than before correction. There is also an area to the northwest of the radar where the signal could not be recovered by the attenuation correction scheme because attenuation was so strong that it completely extinguished the signal. As for Z_{DR}, the attenuation correction is responsible for the radial features seen in some parts of figure 5c, mainly to the northwest of the radar. This is due to the variability of the differential attenuation coefficient from pulse to pulse. In the future we will try to solve this problem by smoothing the differential attenuation coefficient so that the changes from one azimuth to the next are not so sharp.

4. Validation

The self-consistency calibration method is, as mentioned in section 2., based in the fact that in rain the three variables Z_H, Z_{DR} and K_{DP} are not independent. Because of this characteristic, rainfall algorithms (R) for polarimetric radars use pairs of variables such as Z_H-Z_{DR} or Z_{DR}-K_{DP}. This way all the necessary information is kept, while the number of variables used is minimized. Rainfall accumulations as a function of time from the event on the 29 May 2011 are shown in figure 6 (for further details see Evaristo *et al.*, 2011). The blue and red lines are the $R(Z_H,Z_{DR})$ and $R(K_{DP},Z_{DR})$ respectively. In both plots the two lines show very good agreement, which indicates that the calibration method is performing well.

However, this validation procedure only shows that the self-consistency method is working properly. A better way to calibrate would be the comparison with an external source, such as another radar, scanning common areas, whose calibration is known to be correct, or a more classical approach, such as a metal sphere calibration.

The attenuation and differential attenuation correction method is validated by comparing rain accumulations calculated from the radar variables with rain gauges. Even though this method is subject to errors not related to attenuation (the rainfall algorithm), this is at least one indication of the quality of the attenuation correction. The purple line in figure 6 shows the rain accumulation observed by rain gauges in Aurora (figure 6a) and DuPage (figure 6b). The results show a fairly good agreement, considering the ranges at which the two stations are found: 124km for Aurora, 111km for DuPage. These are encouraging results, although not definite. We plan in the future to compare the corrected data from the VU radar to the KLOT data. The KLOT is located 87km to the west of Valparaiso, and is a S-band radar, so attenuation effects are far less important than at C-band. This comparison should provide a more reliable validation of the attenuation scheme.

Acknowledgements:

Funding of this work through MIT Lincoln Laboratory's NEXRAD Enhancements Program for the FAA

6. References

Evaristo, R., Bals-Elsholz, T., Stepanek, A., and Gorgucci, E., 2011: Rainfall estimation with the VU C-band polarimetric radar. *Preprints of the 35th Conference on Radar Meteorology*, Pittsburgh, PA, 26-30 September 2011.

Goddard, J.W.F., J. Tan, and M. Thurai, 1994: Technique for calibration of meteorological radars using differential phase. *Electronics Letters*, 30, 166-167.

Gorgucci, .E., G. Scarchilli, and V. Chandrasekar, 1992: Calibration of radars using polarimetric techniques. *IEEE Transactions on Geoscience and Remote Sensing*, 30, 853-858.

Gorgucci, E., G. Scarchilli, and V. Chandrasekar, 1999: A procedure to calibrate multiparameter weather radar using properties of the rain medium. IEEE Trans. Geosci. Remote Sens., 37, 269–276

Gourley, J.J., A. J. Illingworth and P. Tabary, 2009: Absolute calibration of radar reflectivity using redundancy of the polarization Observations and implied Constraints on drop shapes. *Journal of Atmospheric and Oceanic Technology*, Vol. 26, 689-703.

May, P. T., T. D. Keenan, D. S. Zrnić, L. D. Carey, S. A. Rutledge, 1999: Polarimetric Radar Measurements of Tropical Rain at a 5-cm Wavelength. *J. Appl. Meteor.*, Vol. 38, 750–765.

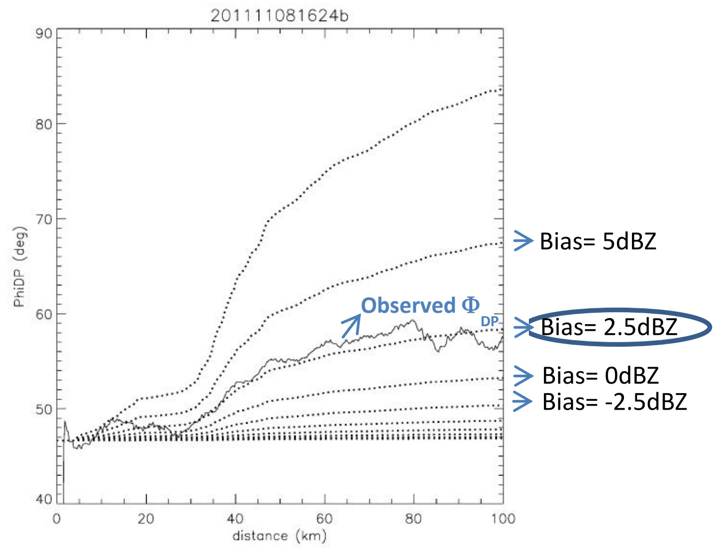

Figure 1. Example of the calibration procedure for one radial of azimuth=331 deg. Observed Φ_{DP} (solid line) and multiple $\Phi_{DP,th}$ (dotted lines) as a function of radar range. The theoretical $\Phi_{DP,th}$ is calculated for different values of Z_H biases to see which value better matches the observed Φ_{DP}.

This particular example shows that the $\Phi_{DP,th}$ closest to the measured multiple Φ_{DP} is the one calculated with a 2.5 dBZ bias in Z_h.

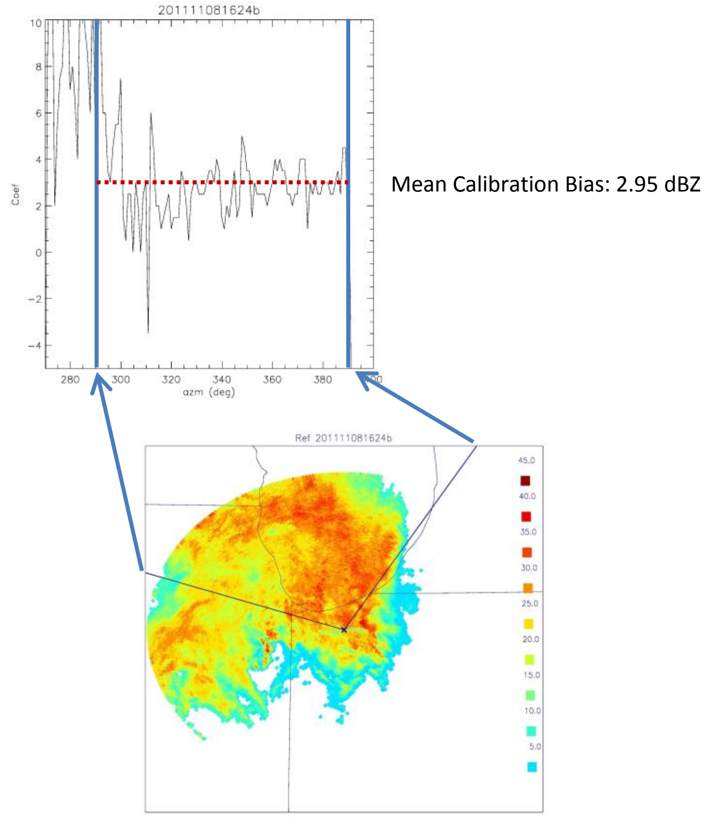

Figure 2. Example of the reflectivity bias as a function of azimuth. We use only the directions where the rainfall is strong enough and the path is mostly filled with precipitation. Ideal conditions would be widespread precipitation all around the radar. For this case we took azimuths between 290° and 30°.

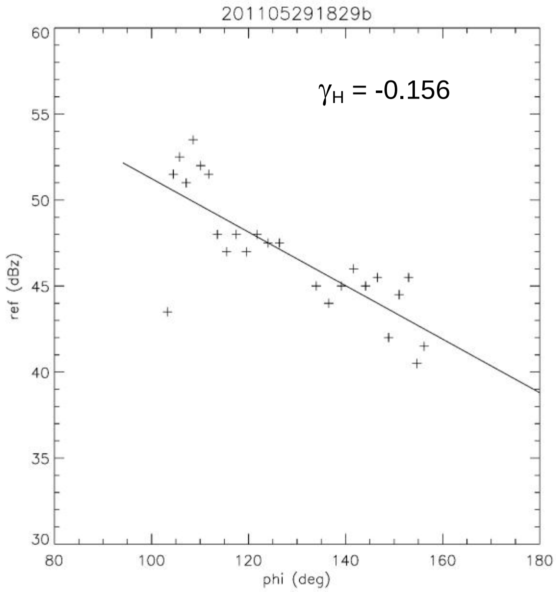

a)

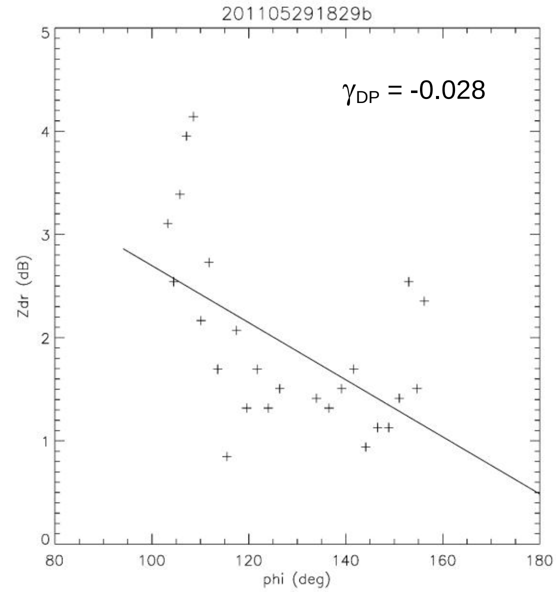

b)

Figure 3. Scatterplots of Φ_{DP} vs Z_H (a) and Z_{DR} (b) and the best fit (calculated from linear regression) for azimuth=275°. The attenuation coefficient (γ_H) and differential attenuation coefficient (γ_{DP}) are the slopes of the fits.

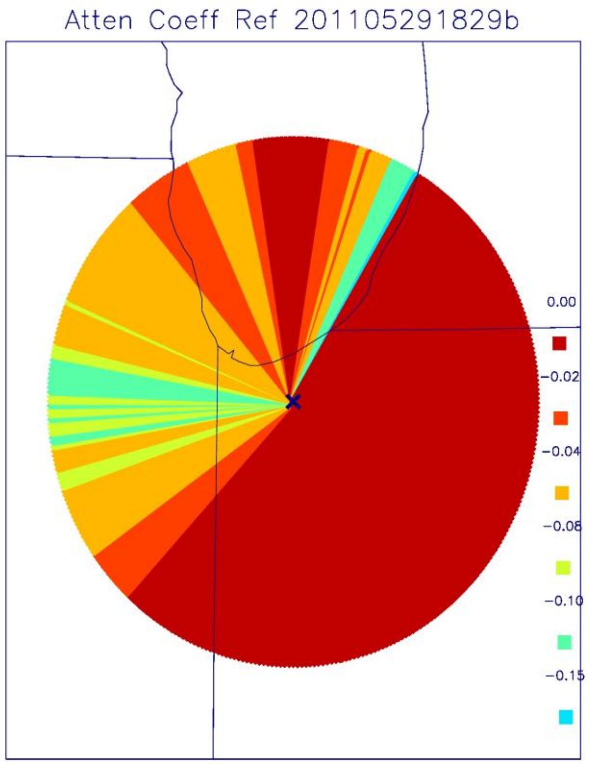

a)

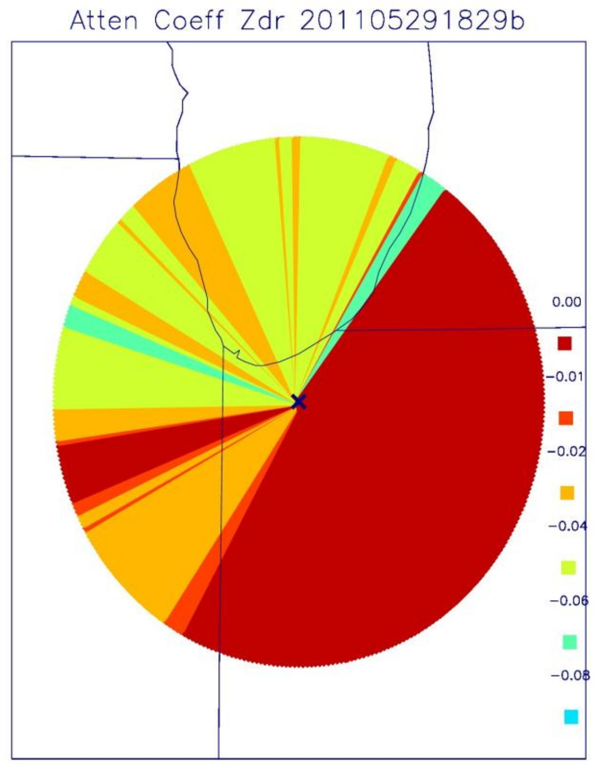

b)

Figure 4. Example of γ_H (a) and γ_{DP} (b) for each azimuth. Note the very low coefficients to the southeast, where there is no precipitation at this point. This is in contrast with the values in the west or northwest where there is convection.

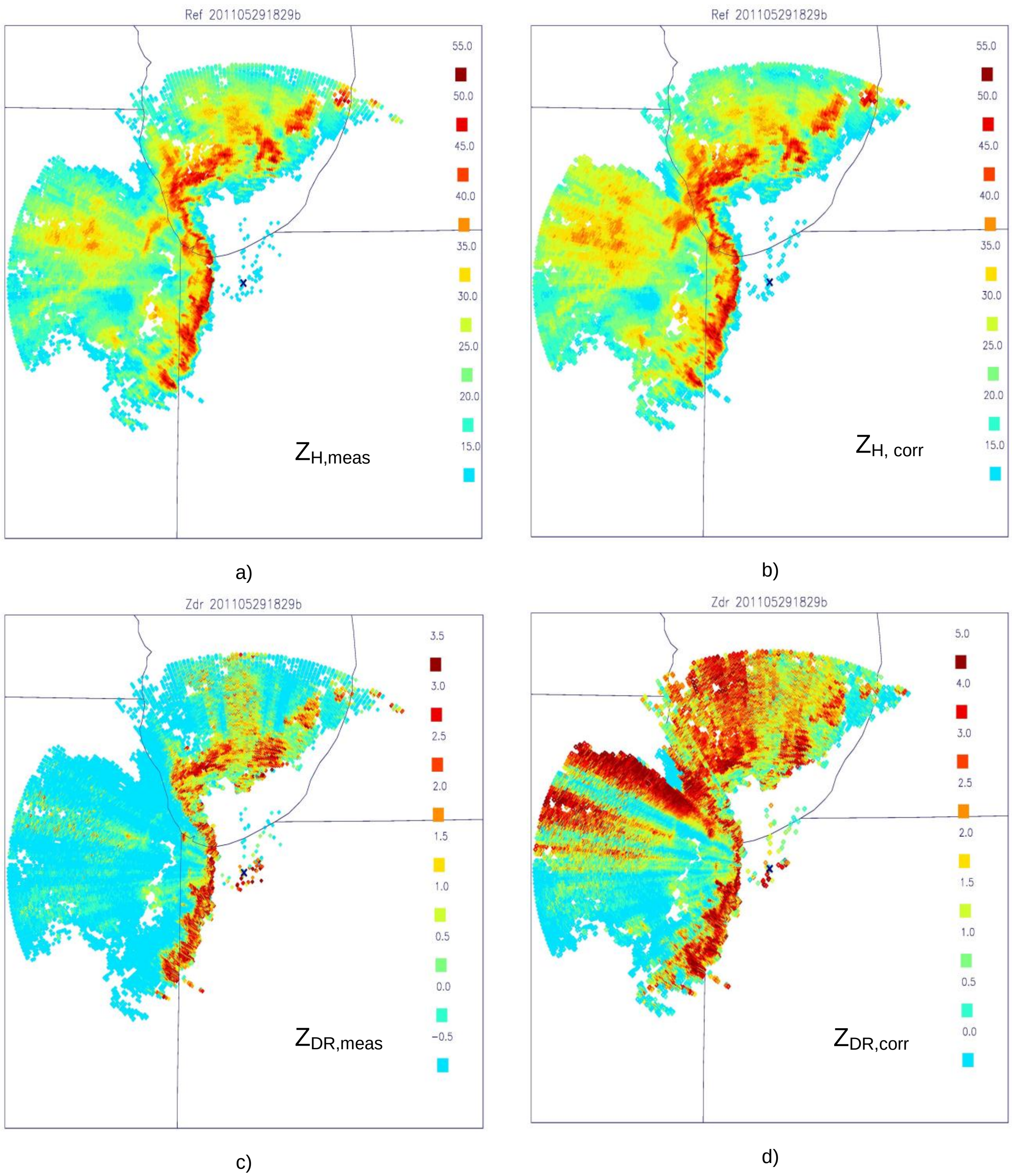

Figure 5. PPI at 1.5° elevation of Z_H and Z_{DR}, before and after attenuation correction.

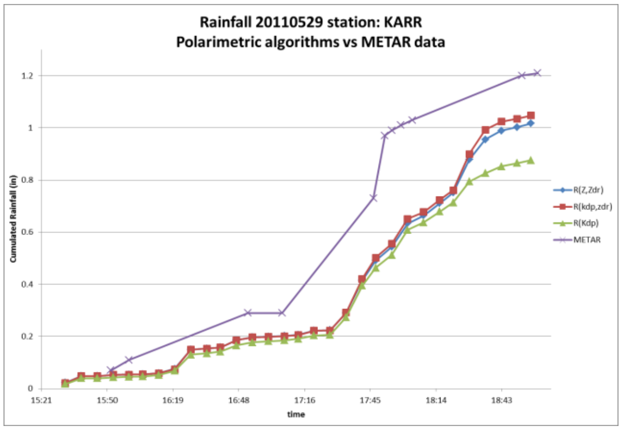

a)

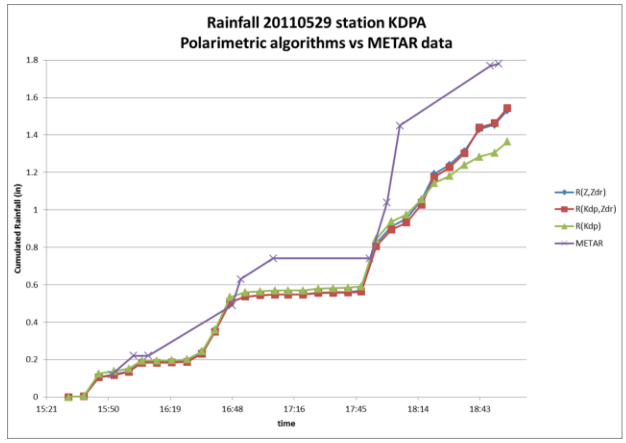

b)

Figure 6. Comparison between rainfall accumulation (in inches) calculated with three polarimetric algorithms ($R(Z_H,Z_{DR})$, $R(K_{DP},Z_{DR})$ and $R(K_{DP})$) and observed in the ground. a) is for Aurora station (KARR) and b) for Du Page (KDPA). The lines show a fairly good agreement, considering that KARR is at a 124km range and KDPA at 111km range from the radar.